

Effect of Al addition on formation and mechanical properties of Mg-Cu-Gd bulk metallic glass

GENG Jia-yuan(耿家源), SUN Yu-feng(孙玉峰), WANG Li-guo(王利国),
ZHU Shi-jie(朱世杰), LIU Li-zhao(刘利召), GUAN Shao-kang(关绍康)

School of Materials Science and Engineering, Zhengzhou University, Zhengzhou 450002, China

Received 19 January 2007; accepted 22 June 2007

Abstract: The effect of partial substitution of Al for Cu on the glass forming ability(GFA) and mechanical properties of $Mg_{65}Cu_{25-x}Al_xGd_{10}$ ($x=0, 1, 3$ and 5 , molar fraction, %) alloys were studied by X-ray diffractometry(XRD), differential scanning calorimetry(DSC) and uniaxial compression test. The result reveals that GFA of the alloys changes slightly with increasing x from 0 to 3 , and then abruptly decreases with x increasing up to 5 . The plasticity can be greatly improved with appropriate substitution of Cu by Al (3% , molar fraction) in $Mg_{65}Cu_{25}Gd_{10}$ bulk metallic glass, and the resultant fracture strength, total strain to failure, and plastic strain are 898 MPa, 2.19% and 0.2% , respectively.

Key words: mg-based bulk metallic glasses; glass forming ability; mechanical properties; plastic strain

1 Introduction

Bulk metallic glasses(BMGs) have attracted considerable research activities due to their high strength, high hardness and excellent resistance against abrasive wear compared with the corresponding crystalline alloys [1–3]. Mg-TM-RE (TM=Cu, Ni, Zn, Ag, Pd and RE stands for rare-earth metal such as Y) alloy systems were reported to exhibit a good glass forming ability(GFA) and high fracture strength, which is more than twice as high as the highest strength of conventional Mg alloys [4–6]. However, Mg-based BMGs fracture in a very brittle manner with almost zero plastic deformation at room temperature[4], which greatly limits their potential applications as structural materials.

Recently, it has been reported that $Mg_{65}Cu_{25}Gd_{10}$ alloy has a significantly improved GFA, enabling the fabrication of the monolithic bulk metallic glass(BMG) with a maximum diameter of 8 mm by the Cu-mold casting method in air[7]. Also, it exhibits the lack of global plasticity at room temperature. The nature of Mg-based BMG's brittleness has become a hot research point. XI et al[8] observed the formation of nanometer-scale damage microvoids on the fracture surface of the

brittle Mg-based BMG, which suggests that plastic deformation might occur. However, it is still very difficult to improve the mechanical properties of Mg-based BMGs.

In order to improve the plasticity, partial substitution of Cu by Ni in the $Mg_{65}Cu_{25}Gd_{10}$ alloy was adapted to fabricate a quaternary $Mg_{65}Cu_{20}Ni_5Gd_{10}$ BMG with the maximum diameter of 5 mm, and it exhibits room temperature plastic strain of about 0.15% under compression tests. The improvement in plasticity may be attributed to intersection between adjacent shear bands [9]. XU et al[10–11] investigated that the addition of Fe element or TiB_2 particle to form Mg-based BMG composites can distinctly improve the plasticity, which mainly attributed to the prohibition of crack propagation by the reinforced particle. AUDEBERT et al[12] reported that a change from brittle to ductile fracture is produced when Cu is partially substituted by Al in $Mg_{65}Cu_{25}MM_{10}$ (MM: mischmetal) alloy, in which they are explained by a reduction of the amount of Cu-rich domains with a chemical short-range-order. These strongly illustrate that the addition of alloying element might be a promising approach to improve the ductility while keeping good GFA.

In the present study, the effect of partial substitution

of Al for Cu on the GFA and mechanical properties of $\text{Mg}_{65}\text{Cu}_{25-x}\text{Al}_x\text{Gd}_{10}$ ($x=0, 1, 3$ and 5 , molar fraction, %) alloys were investigated and the mechanism for the improvement of the mechanical properties was discussed.

2 Experimental

The alloy compositions investigated in the present study were $\text{Mg}_{65}\text{Cu}_{25-x}\text{Al}_x\text{Gd}_{10}$ ($x=0, 1, 3$, and 5 , molar fraction, %). The master ingots of Cu-Gd binary alloy and Cu-Al-Gd ternary alloy were first prepared by arc melting high-purity Cu, Al, Gd under argon atmosphere in a water-cooled copper crucible. Those ingots were then alloyed with Mg (99.99%, mass fraction) in a graphite crucible under a purified argon atmosphere in an induction furnace. The master alloys were re-melted in quartz tubes using induction heating and injected into copper molds with cylindrical cavities of varied diameters from 1 to 9 mm. X-ray diffraction (XRD, Philips PW1700) experiments on the transverse cross-sections of the alloy rods were performed to identify the formation of the amorphous phase in bulk samples by using monochromatic Cu K_α radiation. The microstructural analysis was carried out using a scanning electron microscopy (SEM, Philips Quanta-2000). Thermal analysis of the samples was employed to determine the glass transition temperature, the crystallization temperature and the melting temperature by differential scanning calorimetry (DSC, TA MDSC2920) with a heating rate of 0.333 K/s . The mechanical properties were evaluated by using an Instron 5585 testing machine at a strain rate of $1 \times 10^{-4} \text{ s}^{-1}$. The compression specimens were 4 mm in height and 2 mm in diameter with the ends polished to ensure parallelism. The surface of the fractured specimen was characterized by using SEM.

3 Results

3.1 Phase constitution and microstructure

The phase constitution in $\text{Mg}_{65}\text{Cu}_{25-x}\text{Al}_x\text{Gd}_{10}$ ($x=0, 1, 3$ and 5 , molar fraction, %) alloys was carefully conformed by the X-ray diffractometry. Fig.1 shows the XRD patterns obtained from the transverse cross-sections of the alloy rods with different diameters. For the alloy with $x=0$ in diameter of 8 mm, it exhibits only a broad diffraction peaks in the 2θ range of 30° – 45° , which is characteristic of amorphous structure. It is in agreement with the previous research[7] that fully glassy alloy bulk rods with 8 mm in diameter can be fabricated. With increasing Al content, the maximal diameter for fully glassy bulk rod gradually decreases. For $x=1$ and $x=3$, the diameter of these fully glassy rods is less than 7

mm and 6 mm, respectively. While for $x=5$, the maximal size of fully glassy alloy is largely decreased to 2 mm in diameter.

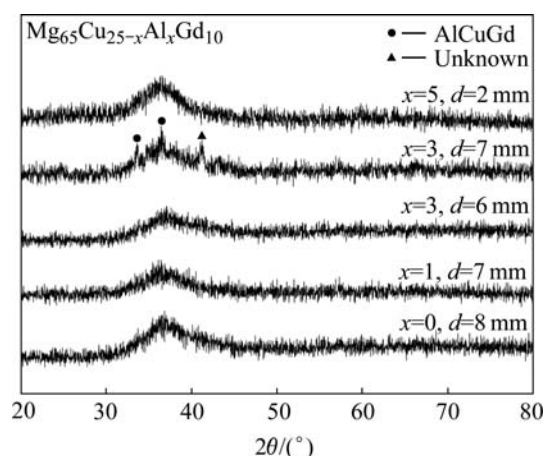


Fig.1 XRD patterns obtained from $\text{Mg}_{65}\text{Cu}_{25-x}\text{Al}_x\text{Gd}_{10}$ BMGs

The X-ray diffraction patterns for the $\text{Mg}_{65}\text{Cu}_{22}\text{Al}_3\text{Gd}_{10}$ alloy with diameter of 7 mm, as indicated in Fig.1, exhibit sharp peaks superimposed on a broad diffraction peak, which is characteristic of crystalline structure. This indicates the coexistence of crystalline and amorphous phases. It can be confirmed that the crystalline phase consists of AlCuGd ternary phase and phase with unknown structure.

The microstructures of the cross-section of the alloy with $x=1$ and $x=3$ in 7 mm diameters are shown in Fig.2. For the alloy with $x=1$, no obvious crystalline phases can be found in the homogenous glass matrix, as shown in Fig.2(a). While for the alloy with $x=3$ shown in Fig.2(b), it exhibits some crystalline phase particles in the matrix, demonstrating that it is easier to form the crystalline phase with increasing Al content of $\text{Mg}_{65}\text{Cu}_{25-x}\text{Al}_x\text{Gd}_{10}$ alloy on the same cooling condition.

3.2 Thermal analysis

Fig.3 shows DSC traces for $\text{Mg}_{65}\text{Cu}_{25-x}\text{Al}_x\text{Gd}_{10}$ glassy alloy rods with diameter of 1 mm. It is found that all the samples exhibit distinct glass transition, followed by a broad super-cooled liquid region and then exothermic reactions due to crystallization. The glass transition temperature(T_g) and crystallization onset temperature(T_x) are indicated by arrows in the DSC traces and summarized in Table 1. For the alloy with $x=0$, the T_g and T_x are 414 K and 482 K, respectively. With increasing x , the glass transition temperature slightly increases from 415 K at $x=1$ to 416 K at $x=3$, and finally increases up to 420 K at $x=5$. Furthermore, the crystallization onset temperature gradually decreases from 472 K to 463 K with increasing x from 1 to 5. As a result, the super-cooled liquid regions ($\Delta T_x = T_x - T_g$) decreases from 68 K to 57 K with increasing x from 0 to

Table 1 Thermal analysis results (T_g , T_x , T_m and T_l), GFA parameters (ΔT_x and T_{rg}) and glass forming maximum diameters(D_{max}) for $Mg_{65}Cu_{25-x}Al_xGd_{10}$ BMGs

x	T_g/K	T_x/K	T_m/K	T_l/K	$\Delta T_x/K$	T_{rg}	D_{max}/mm
0	414	482	676	732	68	0.565	8
1	415	472	685	742	57	0.559	7
3	416	470	686	745	54	0.558	6
5	420	463	690	762	43	0.551	2

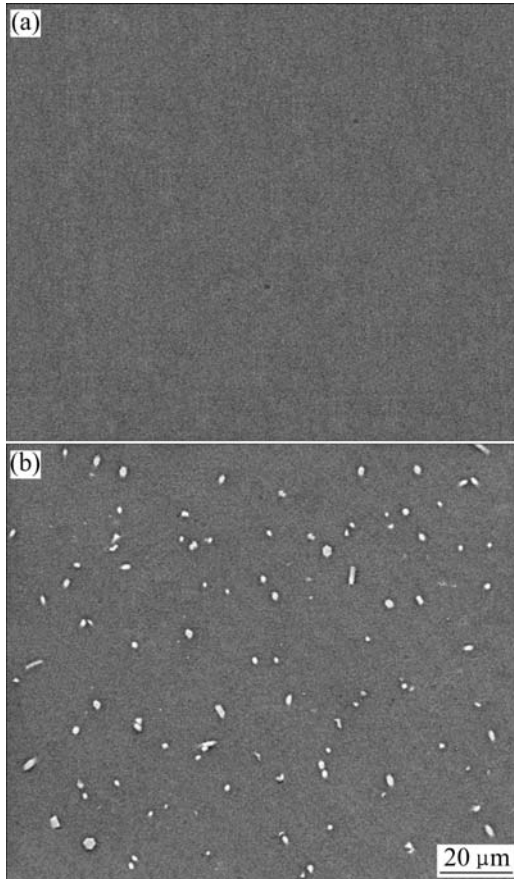


Fig.2 SEM image showing microstructures of $Mg_{65}Cu_{25-x}Al_xGd_{10}$ alloy with diameter of 7 mm: (a) $x=1$; (b) $x=3$

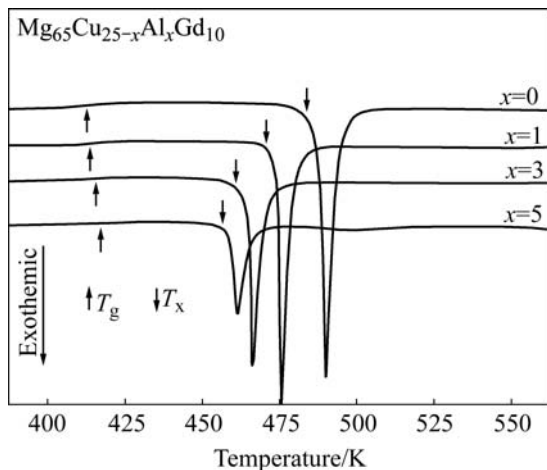


Fig.3 DSC traces obtained from $Mg_{65}Cu_{25-x}Al_xGd_{10}$ BMGs

1, then continuously decreases to 54 K for $x=3$ and 43 K for $x=5$. It is well known that higher ΔT_x value means higher glass-forming ability[13], indicating that the super-cooled liquid can exist in a wide temperature range and has higher barrier to the nucleation and growth of the competing crystalline phases. A partial substitution of Cu by Al in $Mg_{65}Cu_{25-x}Al_xGd_{10}$ alloys decreases the thermal stability of super-cooled liquid, thereby results in the decrease of GFA.

Fig.4 shows the endothermic curve for melting of the $Mg_{65}Cu_{25-x}Al_xGd_{10}$ glassy alloy rods with diameter of 1 mm during continuous heating in the DSC. The onset and end melting temperatures (T_m and T_l) are marked by arrows in the DSC traces and summarized in Table 1, respectively. T_m and T_l for the alloy with $x=0$ are 676 K and 732 K, respectively, and the melting range of the glassy alloy is about 56 K. With x increasing, T_m and T_l slightly increase from 685 K and 742 K at $x=1$ to 686 K and 745 K at $x=3$, respectively, and the corresponding melting region of the glassy alloys slightly increases to 57 K and 59 K. With increasing x up to 5, T_m of the glassy alloy slightly increases to 690 K; while T_l of the glassy alloy significantly increases to 762 K, resulting in the melting range increases to 72 K. The reduced glass transition temperature T_{rg} ($T_{rg}=T_g/T_l$) value is employed to present the forming ability of the amorphous phase in the temperature range between T_l and T_g . In order to get a glass transition during solidification, the formation of the competing crystalline phase should be prevented in the temperature range between T_l and T_g . Higher T_{rg} value indicates that competing crystalline phase can be restrained to form glassy phase at relatively low cooling rate, resulting in the high glass-forming ability[14]. With Al content increasing from 0 to 5%, T_{rg} decreases from 0.565 to 0.551, leading to the decrease in GFA.

3.3 Compressive properties

Fig.5 shows the stress—strain curves of the bulk glassy $Mg_{65}Cu_{25-x}Al_xGd_{10}$ alloy rods with a diameter of 2 mm after compression test. The ultimate compressive fracture strength(σ_f) and compressive fracture total strain (ϵ_f) of the alloy with $x=0$ are 837 MPa and 1.8%, respectively, and the plastic strain is almost zero. With

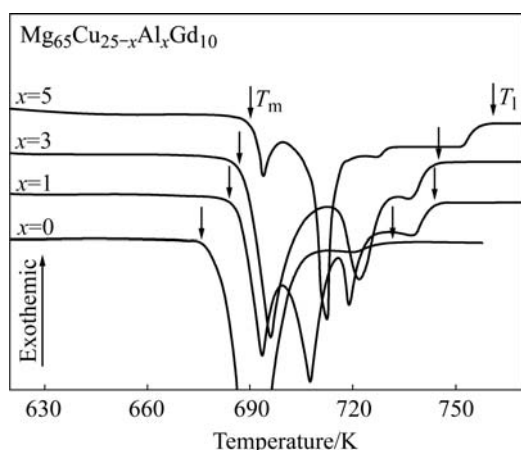


Fig.4 DSC traces showing melting endotherms obtained from $\text{Mg}_{65}\text{Cu}_{25-x}\text{Al}_x\text{Gd}_{10}$ BMGs

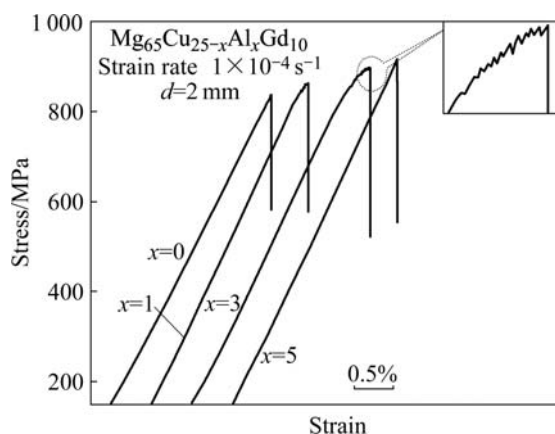


Fig.5 Compressive stress—strain curves of $\text{Mg}_{65}\text{Cu}_{25-x}\text{Al}_x\text{Gd}_{10}$ BMGs

partial substitution of Cu by 1% Al, σ_f and ε_f increase to 863 MPa and 1.92%, respectively, but it still has no distinct macroscopic plastic strain. When increasing Al content to 3%, the alloy exhibits compressive elastic strain(ε_e) of 1.99% and plastic strain(ε_p) of about 0.2%. This reveals that the plastic deformation occurs under compressive loading. The σ_f and ε_f of the alloy with $x=3$ are 898 MPa and 2.19%, respectively, which are higher than those of the alloy with $x=0$ and $x=1$. The inset in Fig.4 exhibits the enlarged serrated flow on the stress—strain curves of the alloy with $x=3$, showing that dozens of serrations appear before the failure occurs. The serrated flow phenomenon indicates that the plastic deformation of the BMGs occurs by generation and propagation of shear bands[15]. However, for the alloy with $x=5$, the compressive fracture strength continuously increases to 915 MPa, but the plastic strain almost decreases to zero.

3.4 Fracture characteristics

Fig.6 shows the fractographic appearance of the

monolithic BMG with different Al contents after compression test. As shown in Fig.6(a), only few shear bands can be observed on the fracture surface of the alloy with $x=0$, indicating that the deformation occurs through a shear fracture mode[11]. Usually fracture occurs accompanied with the formation of crack shown in Fig.6(a), which has been reported for the most of the Mg-based BMGs. Compared with the fracture morphology of the alloy with $x=0$, the fracture surface of the alloy with $x=1$ exhibits more shear bands, but the distinct crack is generated, indicated by row in Fig.6(b). For the alloy with $x=3$, the fracture surface presented in Fig.6(c) exhibits multiple shear bands and no distinct crack. These well-developed shear bands indicate the occurrence of drastic shear deformation under a uniaxial compressive load. Fig.6(d) shows that the fracture surfaces of the alloy with $x=5$ consist of smooth regions and few shear bands. The smooth region results from fast shear sliding that reflect the brittle fracture mode.

On the other hand, it can be seen from Fig.6(a) that the shear bands for the alloy with $x=0$ are almost parallel to the shear stress direction, indicating rapid propagation of shear bands and subsequent occurrence of brittle fracture without distinct plastic deformation. As for the alloy with $x=3$, some adjacent shear bands intersect with each other, which is marked with a circle in Fig.6(c), indicating that the plastic deformation occurs[9].

4 Discussion

4.1 Effect of Al addition on BMG formation

With increasing Al content in $\text{Mg}_{65}\text{Cu}_{25-x}\text{Al}_x\text{Gd}_{10}$ alloys, the maximal size of fully glassy alloy rods is gradually decreased. The melting range increases from 56 K for the alloy with $x=0$ to 72K for the alloy with $x=5$. It is suggested that the composition of alloy with $x=5$ is much farther away from the eutectic composition as compared with the alloy with $x=0$, 1 and 3, which implies that the addition of 5%Al remarkably decreases the GFA of the $\text{Mg}_{65}\text{Cu}_{25-x}\text{Al}_x\text{Gd}_{10}$ BMG.

During the formation of BMG, it exhibits the competitive growth of crystalline phase and amorphous phase. In the $\text{Mg}_{65}\text{Cu}_{25-x}\text{Al}_x\text{Gd}_{10}$ alloys, with the increase of Al content, the crystalline phase is easier to form at the same cooling rate. Since Al is very active and has a strong tendency to form intermetallic compound with other metals, the addition of Al element in $\text{Mg}_{65}\text{Cu}_{25}\text{Gd}_{10}$ alloy can induce the precipitation of crystalline phase, i.e., AlCuGd in this study. With increasing Al content, the formation of amorphous phase is restrained, therefore the GFA decreases.

4.2 Improvement of plasticity

Compared with most of the previously reported

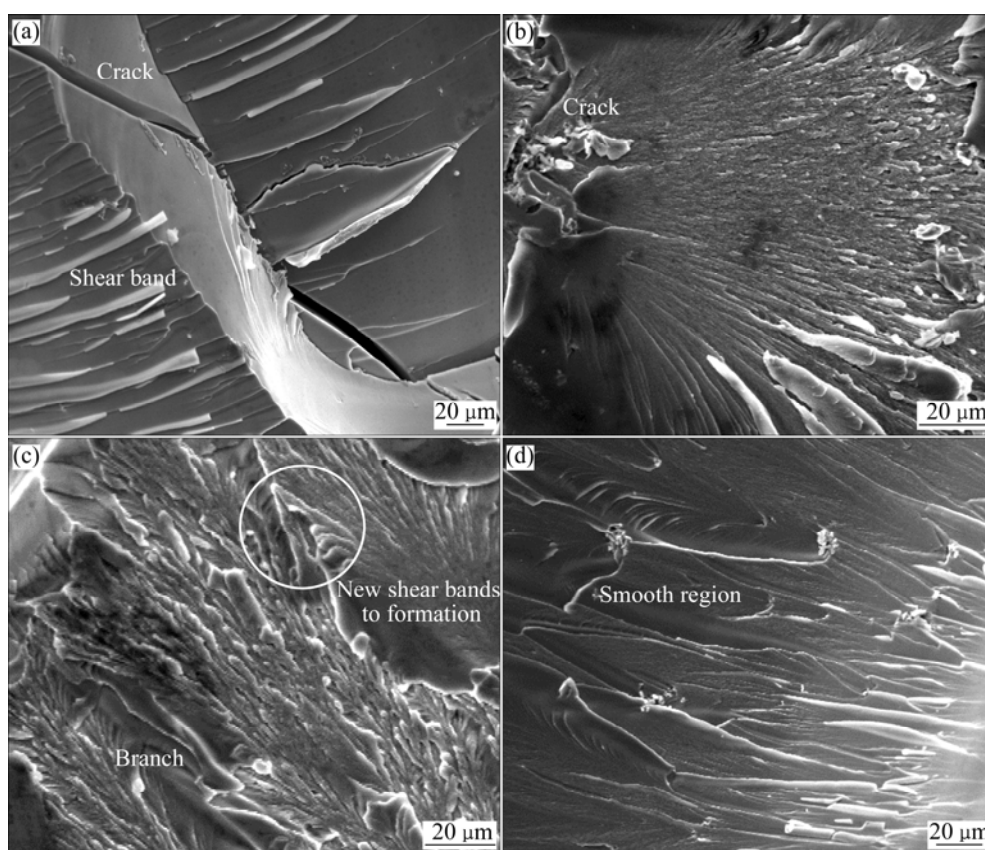


Fig.6 SEM images showing fracture surface morphologies of $\text{Mg}_{65}\text{Cu}_{25-x}\text{Al}_x\text{Gd}_{10}$ BMGs: (a) $x=0$; (b) $x=1$; (c) $x=3$; (d) $x=5$

Mg-based BMGs, $\text{Mg}_{65}\text{Cu}_{22}\text{Al}_3\text{Gd}_{10}$ BMG exhibits plastic deformation under compressive loading, demonstrating that substitution of Cu by Al can greatly improve the plasticity of $\text{Mg}_{65}\text{Cu}_{25}\text{Gd}_{10}$ BMG. Since the difference in atomic radius between Al-Mg and Al-Gd is smaller than that of Cu-Mg and Cu-Gd[16], an appropriate substitution of Cu by Al breaks the densely packed structure and increases the amount of free volume, therefore, multiple shear bands is easier to form through the coalescence of the free volume for the alloy with $x=3$ [17]. It is noted that each shear band refers to single serration on the stress—strain curve, and therefore the formation of these multiple shear bands can also be reflected on the stress—strain curves shown in Fig.5[18].

With the formation of multiple shear bands, some adjacent shear bands intersect with each other, resulting in the phenomenon that the further propagation is difficult to occur. When further increasing compressive loading, the new shear bands will be initiated and the shear bands may branch along different directions, as indicated by white arrows in Fig.6(c). The stress will distribute more uniformly throughout the materials and avoid highly the localization of shear stress. Therefore, the propagation of only one or a few shear bands inside the whole sample is prohibited, leading to the improvement in the ductility.

It is also noted that the alloy with $x=0$ exhibits no distinct macroscopic plastic deformation before fracture, as shown in Fig.4, which might be attributed to the embrittlement resulted from the structural relaxation at room temperature[9]. As a result, the cracks form easily and propagate quickly under compressive stress, subsequently resulting in the occurrence of failure. In Fig.6(a), a crack can be observed. Comparatively, there is little crack on the compressive fracture surface for the alloy with $x=3$, as clearly shown in Fig.6(c). The addition of the alloying element Al can increase glass transition temperature, which reflects the enhancement of bonding force among these constituent atoms and might result in the improvement of stability against structural relaxation, therefore, the crack initiation and propagation could be suppressed and the distinct plastic deformation occurs under compressive loading. It is the most likely reason for improvement in ductility and strength through partial substitution of Cu by 3% Al in the $\text{Mg}_{65}\text{Cu}_{25-x}\text{Al}_x\text{Gd}_{10}$ BMG.

5 Conclusions

1) With increasing x , the super-cooled liquid region decreases from 68 K to 43 K. The melting temperature region significantly increases when increasing x to 5,

indicating that the composition of the alloy with $x=5$ is farther away from the eutectic composition points as compared with the alloy with $x=0-3$, thereby distinctly decreasing the GFA.

2) Mg₆₅Cu₂₂Al₃Gd₁₀ BMG with diameter of 6 mm is successfully fabricated by conventional Cu-mold casting method. Compared with most of the previously reported Mg-based BMGs, it exhibits plastic deformation under compressive loading, demonstrating that substitution of Cu by Al can greatly improve the plasticity of Mg₆₅Cu₂₅Gd₁₀ BMG. The improvement might be attributed to the fact that the addition of Al promotes the formation of multiple shear bands and suppresses the crack initiation and propagation during compressive stress. The compressive fracture strength and plastic strain increase to 898 MPa and 0.2%, respectively.

Acknowledgments

The authors would like to express heartfelt thanks to Prof. Zhang Tao and his co-workers, Beijing University of Aeronautics and Astronautics, for their preparing the BMG samples.

References

- [1] INOUE A, OHTERA K, KITA K, MASUMOTO T. New amorphous Mg-Ce-Ni alloys with high strength and good ductility [J]. Japanese Journal of Applied Physics, 1988, 27(12): L2248-L2251.
- [2] SUN Yu-feng, WANG Yu-ren, WEI Bing-chen, LI Wei-huo, SHEK Chung-hong. Effect of carbon addition on microstructure and mechanical properties of Ti-based bulk metallic glass forming alloys [J]. Trans Nonferrous Met Soc China, 2005, 15(4): 727-732.
- [3] KONG Jian, XIONG Dang-sheng, YUAN Qun-xing, YE Zhi-tao. Strengthening bulk metallic glasses with minor alloying additions [J]. Trans Nonferrous Met Soc China, 2006, 16(s2): s598-s602.
- [4] AMIYA K, INOUE A. Thermal stability and mechanical properties of Mg-Y-Cu-M (M=Ag, Pd) bulk amorphous alloys [J]. Materials Transactions, 2000, 41(11): 1460-1462.
- [5] PARK E S, KANG H G, KIM W T, KIM D H. The effect of Ag addition on the glass-forming ability of Mg-Cu-Y metallic glass alloys [J]. Journal of Non-Crystalline Solids, 2001, 279(2/3): 154-160.
- [6] MA H, MA E, XU J. A new Mg₆₅Cu_{7.5}Ni_{7.5}Zn₅Ag₅Y₁₀ bulk metallic glass with strong glass-forming ability [J]. J Mater Res, 2003, 18(10): 2288-2291.
- [7] MEN H, KIM D H. Fabrication of ternary Mg-Cu-Gd bulk metallic glass with high glass-forming ability under air atmosphere [J]. Journal of Materials Research, 2003, 18(7): 1502-1504.
- [8] XI X K, ZHAO D Q, PAN M X, WANG W H, WU Y, LEWANDOWSKI J J. Fracture of brittle metallic glasses: Brittleness or plasticity [J]. Physical Review Letters, 2005, 94(12): 125510.
- [9] YUAN Guang-yin, INOUE A. The effect of Ni substitution on the glass-forming ability and mechanical properties of Mg-Cu-Gd metallic glass alloys [J]. Journal of Alloys and Compounds, 2005, 387(1/2): 134-138.
- [10] MA H, XU J, MA E. Mg-based bulk metallic glass composites with plasticity and high strength [J]. Appl Phys Lett, 2003, 83(14): 2793-2795.
- [11] XU Ying-kun, MA Han, XU Jian, MA En. Mg-based bulk metallic glass composites with plasticity and gigapascal strength [J]. Acta Materialia, 2005, 53(6): 1857-1866.
- [12] AUDEBERT F, ROZENBERG S, GALANO M. Rapidly quenched Mg₆₅Al_xCu_{25-x}MM₁₀ (MM: mischmetal) alloys [J]. Journal of Non-Crystalline Solids, 2001, 287(1/3): 45-49.
- [13] INOUE A, ZHANG T, MASUMOTO T. Glass-forming ability of alloys [J]. Journal of Non-Crystalline Solids, 1993, 156/158: 473-480.
- [14] WANIUK T A, SCHROERS J, JOHNSON W L. Critical cooling rate and thermal stability of Zr-Ti-Cu-Ni-Be alloys [J]. Applied Physics Letters, 2001, 78(9): 1213-1215.
- [15] HUFNAGEL T C, EL-DEIRY P, VINCI R P. Development of shear band structure during deformation of a Zr₅₇Ti₅Cu₂₀Ni₈Al₁₀ bulk metallic glass [J]. Scripta Materialia, 2000, 43(12): 1071-1075.
- [16] TAKEUCHI A, INOUE A. Classification of bulk metallic glasses by atomic size difference, heat of mixing and period of constituent elements and its application to characterization of the main alloying element [J]. Materials Transactions, 2005, 46(12): 2817-2829.
- [17] SHEK C H, LIN G M. Dilatometric measurements and calculation of effective pair potentials for Zr₄₁Ti₁₄Cu_{12.5}Ni₁₀Be_{22.5} bulk metallic glass [J]. Materials Letters, 2003, 57(5/6): 1229-1232.
- [18] SUN Y F, SHEK C H, GUAN S K, WEI B C, GENG J Y. Formation, thermal stability and deformation behavior of graphite-flakes reinforced Cu-based bulk metallic glass matrix composites [J]. Mater Sci Eng A, 2006, 435/436: 132-138.

(Edited by YANG Bing)